COBEM 2021 26th International Congress of Mechanical Engineering
November 22-26, 2021, Virtual Congress, Brazil
ABCM Associação Brasileira de Engenharia e Ciências Mecânicas

# COB-2021-1411
# Simulation and Performance analysis of a Hybrid Rocket Engine with self-pressurizing Oxidizer

**Bruno Pinto Costa**
**Alexandre Costa Goulart**
**Gabriel Lopes Yamato**
**Calvin Souto Trubiene**
**João Pedro Vilas Boas Silva**
**Isabella De Salvo Fontoura**
**Matheus Andrucioli de Carvalho Cruz**
**Matheus Bello de Paula**
**Victor Nicoláo Capacia**
PION Labs Engenharia LTDA, Vila Prudente, São Paulo, SP
Vila Prudente, São Paulo/SP - Brazil
bruno@pionlabs.com.br
alexandrecgoulart@gmail.com

***Abstract.*** *There are many challenges to simulate and design a hybrid engine, such as the dimensioning of the feed lines and tanks, propulsive performance calculations, and simulations of the expected behavior in the combustion chamber and the oxidizer tank during the engine operation. In this work, methods are assembled in a concise and complete analysis of the Gluon hybrid rocket engine, developed by PION Labs, with a blowdown pressurization system, using $N_2O$ as oxidizer and a paraffin-based fuel. For that, a study will be presented on the peculiar characteristics of the oxidizer and its behavior during the phases of operation of the rocket engine. Then, the main equations that describe the operation of the rocket engine, including the combustion chamber, injection plate, feed lines, and the oxidizer tank are presented, and the performance indicators calculations of the engine are shown and discussed. Finally, simulation results of the combustion chamber and the oxidizer tank during engine firing will be presented, leading to the concluding remarks on the data obtained.*

***Keywords:*** *Hybrid Rocket Engine, Rocket Propulsion, Nitrous Oxide, Rocket Motor Simulation*

## 1. INTRODUCTION

Chemical Rocket engines can be classified according to the physical state of the propellant pair: solid, liquid, and hybrid. In a hybrid propulsion system, the oxidizer and fuel are stored in separate compartments and are in different physical states. Usually, the oxidizer is stored in a liquid phase and the fuel in a solid phase. This architecture retains a specific impulse of reasonably high performance while presenting a simpler hydropneumatic configuration compared to liquid propellant engines and also safer storage and handling compared to solid propellants. It is common to use nitrous oxide as a rocket propellant in many hybrid space vehicles, due to it being readily available and due to the ease of operation with it, in addition to being self-pressurizing at room temperature, making it unnecessary to use an additional pressurizing tanks, thus decreasing the total mass and cost of the system.

In operations with a self-pressurized oxidizer it is possible either to close the main oxidizer valve when the liquid phase ***"LP"*** is depleted or keep the valve open to vent vapour through the combustion chamber, which can be denoted as the vapor phase ***"VP"*** of the thruster. An advantage presented by the second configuration is the possibility to burn the remaining pressurizing vapor after the liquid oxidizer is depleted. This can be achieved letting the main valve open, which will let the vapor consume any remaining fuel, part of the fuel supporting structure or even the surface of the thermal liner. Burning the remaining vapor gives hot gases that can keep the combustion chamber pressurized and thus more efficiently eject the remaining mass. Differently from the *LP*, the *VP* is inherently unsteady, thus, one of the objectives of the developed simulation is to give a quantitative evaluation of this mode of operation.

A complete and accurate simulation of hybrid rocket engines is an important tool in engine development, reducing costs with additional testing and lessening the probability of unexpected failures at the test bench, which can lead to

redesigns. Another important factor is the possibility to adjust simulations to data gathered in tests, which, for hybrid engines, is related in special to combustion efficiency, that can vary widely depending on engine design. All these aspects have led the development of the presented code and are its main objectives, serving as a comprehensive tool for hybrid rocket design.

## 2. METHODOLOGY

### 2.1 Propulsion System Overview

The Quark vehicle is propelled by the Gluon FT (Full Thrust) Hybrid Rocket Motor which uses Nitrous Oxide ($N_2O$) as oxidizer and Paraffin Wax ($C_{32}H_{66}$) as fuel with and additive of $2\%$ carbon black (PWCB-2) as an opacifier. The "Full Thrust" designation comes from the fact that it's expanding the capability of the design developed with the Gluon hybrid rocket technology demonstrator, which had an extensive test campaing.

In Figure 1 a section view is shown where, at the left there is the oxidizer thank and venting valve, at the middle there is the control assembly for automated oxidizer loading and engine control. On the right side, the combustion chamber is visible.

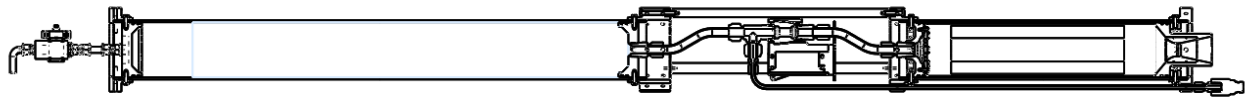

Figure 1. Side section view of the Gluon FT hybrid engine.

The engine specifications were determined in order to meet the requirements of the Quark vehicle, which is capable of launching multiple scientific and educational experiments in atmospheric flight at each launch. General specifications are presented in Table 2.1

| **Gluon FT - General Specifications** | |
|---|---|
| $Thrust$ | $1.0\ kN$ |
| $O/F\ ratio$ | 5.0 |
| $t_{burn}$ | $5.0\ s$ |
| $P_C$ | $24.1\ bar\ (350\ psi)$ |

Table 1. General specifications of the Gluon FT engine considered in it's conception.

### 2.2 Computational Method

For this work, a tool in Python programming language was developed, which is able to simulate the transient behavior of the combustion chamber of a Hybrid Rocket Engine. Along with it, another code was integrated, also in python, which simulates the behavior of a blowdown feed system with a self-pressurizing oxidizer.

#### 2.2.1 Combustion Chamber Model

The equation that describes the behavior of the thruster's combustion chamber pressure is presented by (Eilers and Whitmore, 2008). This equation is derived from the mass balance and is described in equation 1. This differential equation was solved using Euler's first-order numerical method.

$$\frac{\partial p}{\partial t} = \frac{R \cdot T_0}{V_c} \cdot (\dot{m}_{fuel} + \dot{m}_{oxi} - \dot{m}_{nozzle}) - \frac{p}{V_c}\frac{\partial V_c}{\partial t}, \tag{1}$$

Where $p$ is the pressure in the combustion chamber, $t$ is the thruster operating time, $R$ is the gas constant, $T_0$ is the stagnation temperature, $V_c$ is the combustion chamber volume , $\dot{m}_{fuel}$ is the mass flow of fuel, $\dot{m}_{oxi}$ is the mass flow of oxidizer, and $\dot{m}_{nozzle}$ is the nozzle mass flow.

As the fuel is consumed, the combustion chamber volume increases with time, that is, $V_c$ depends of the fuel mass flow. According to (Sutton and Biblarz, 2016) the fuel mass flow depends on the propellant burning area ($A_b$), the fuel grain density ($\rho_{fuel}$) and the regression rate($\dot{r}$). Equation 2 describes fuel mass flow behavior.

$$\dot{m}_{fuel} = A_{burn} \cdot \rho_{fuel} \cdot \dot{r}, \tag{2}$$

$$\dot{r} = a \cdot \left(\frac{\dot{m}_{oxi}}{\pi \cdot r^2}\right)^n \tag{3}$$

Where $a$ and $n$ are ballistics coefficients and depends of the propellant pair, and $r$ is fuel grain port radius.

The equation 4 shows the nozzle mass flow .

$$\dot{m}_{nozzle} = p \cdot A_t \cdot \gamma \cdot \sqrt{\frac{[2/(\gamma+1)]^{(\gamma+1)/(\gamma-1)}}{\sqrt{\gamma R T_0}}} \tag{4}$$

Where $\gamma$ is the ratio of specific heats and $A_t$ is the nozzle throat area.

### 2.2.2 Blowdown self-pressurization Model

Multiple thermodynamic methods are needed for the simulation and are applied in the appropriate conditions and modified as needed. Each one of which were used as base to the developing the code are presented next.

**Incompressible Model**

For propellants considered quasi-incompressible liquids, the oxidizer mass flow in the injector can be calculated using equation 5. This model considers that the mass flow in the injector is single-phase and the density is constant.

$$\dot{m}_{inc} = A_c \cdot C_d \cdot \sqrt{2 \cdot \rho_1 \cdot (P_1 - P_2)}, \tag{5}$$

Where $A_c$ is the cross-sectional area of the orifice, $C_d$ is the discharge coefficient, $P_2$ is the downstream pressure, $\rho_1$ and $P_1$ are, respectively, the upstream density and pressure.

**HEM Model**

Often in self-pressurized propellants, such as nitrous oxide ($N_2O$), the static pressure is very close to the saturation pressure. In this case, when accelerating the liquid inside the injector, the static pressure can achieve values below the vapor pressure, and instantaneous vaporization and cavitation can occur. As a result, the mass flow through the injector will be limited. (Waxman *et al.*, 2013) shows a model to predict the two-phase critical flow through an injector. Equation 6 shows this model, called the Homogeneous Equilibrium Model (HEM).

$$\dot{m}_{HEM} = A_c \cdot C_d \cdot \rho_2 \cdot \sqrt{2 \cdot (h_1 - h_2)}, \tag{6}$$

The HEM assumes thermal equilibrium and same velocity between the liquid and vapor phases, and the isentropic flow across the injector ($s_1 = s_2$). $\rho_2$ represents downstream density, $h_1$ is the upstream specific enthalpy, and $h_2$ is the downstream specific enthalpy.

**NHNE Model**

(Dyer *et al.*, 2007) proposed to merge the incompressible model with the homogeneous equilibrium model, doing the weighted average of these two models. This new model is called Nonhomogeneous Nonequilibrium (NHNE) and it is shown in equation 8. The NHNE considers that the longer the oxidizer remains inside the injector, the longer it has to vaporize. For this, the non-equilibrium parameter($k$) is used, which depends on the ratio between the bubble growth time($\tau_b$) and the fluid residence time($\tau_r$).

$$k = \frac{\tau_b}{\tau_r} = \sqrt{\frac{P_1 - P_2}{P_v - P_2}}, \tag{7}$$

$$\dot{m}_{NHNM} = A_c \cdot \frac{(\dot{m}_{inc}/A_c) + k \cdot (\dot{m}_{HEM}/A_c)}{1+k}, \tag{8}$$

Where $P_v$ is the fluid vapor pressure.

**Adiabatic Two-Phase Entropy Model**

Nonhomogeneous Nonequilibrium Model (NHNE), developed by (Whitmore and Chandler, 2010), is used. This model considers that the system's total entropy is constant, that is, the sum of the entropy that leaves the tank plus the entropy inside the tank remains always constant.

Other 5 assumptions are used in this model.

**1 -** The tank is small and, therefore, the pressure instantly equalizes inside the tank during the evacuation;

**2 -** There is no heat transfer to the fluid during the evacuation process;

**3 -** Inside the tank, the fluid is stratified with distinct layers of liquid and vapor;

**4 -** The hydrostatic pressure of the fluid is considered to be null when compared to the saturation vapor pressure;

**5 -** Inside the oxidizer tank liquid and vapor phases are well divided, meaning that vapor will only be ejected after the liquid phase is depleted. While there is still liquid oxidizer in the tank, if pressure decreases enough along the feed line, the fluid is considered to vaporize in the feed line.

The code developed is iterative and queries at all times the nitrous oxide database present on the NIST (National Institute of Standards and Technology) website.

Given the initial temperature and pressure of the $N_2O$, the initial liquid saturated density $(\rho_l)$ and initial vapor saturated density $(\rho_v)$ are calculated by interpolation of the NIST. And after that, the title $(X)$ is calculated.

$$X = \frac{(\rho_v \cdot \rho_l) - \rho_v \cdot \rho_0}{\rho_0 \cdot (\rho_v - \rho_l)} = \frac{(\rho_v \cdot \rho_l) - \rho_v \cdot (m_0/V_{tank})}{(m_0/V_{tank}) \cdot (\rho_v - \rho_l)} \tag{9}$$

Knowing the value of $X$, it is possible to calculate the initial specific entropy $(s_0)$ using the Equation 10. $s_v$ and $s_l$ are the specific entropy of the vapor and liquid respectively, $V_{tank}$ is the volume of the entire oxidizer tank, $m_0$ is the initial mass of fluid in tank and $\rho_0$ is the initial total density of fluid in tank. Then, the initial total entropy of the tank $(S_0)$ can be calculated by multiplying initial mass with the initial specific entropy.

$$s_0 = s_l \cdot (1 - X) + s_v \cdot X \tag{10}$$

$$S_0 = m_0 \cdot s_0 \tag{11}$$

While there is liquid oxidizer inside the tank, the $N_2O$ mass flow is calculated using the NHNE model, as shown in Equation 12. Where $A_{out}$ is the tank-outlet area and $\dot{m}_{l,out}$ is the liquid oxidizer mass flow through the outlet. This equation admits that the output fluid is liquid and only after the injector the fluid can turn into vapor.

$$\dot{m}_{oxi} = \dot{m}_{l,out} = A_{out} \cdot \frac{(\dot{m}_{inc}/A_c) + k \cdot (\dot{m}_{HEM}/A_c)}{1+k} \tag{12}$$

Through the time interval $(\Delta t)$, it is possible to calculate the new quantities in the next step (i + 1). As shown in the equations 13 to 16:

$$S_{i+1} = S_i - (\dot{m}_{l,out} \cdot s_l) \cdot \Delta t \tag{13}$$

$$m_{i+1} = m_i - \dot{m}_{l,out} \cdot \Delta t \tag{14}$$

$$\rho_{i+1} = \frac{m_{i+1}}{V_{tank}} \tag{15}$$

$$s_{i+1} = \frac{S_{i+1}}{m_{i+1}} \tag{16}$$

Where $i$ is the iteration time index

Iteratively, using the NIST property tables it is possible to calculate the current mass of vapor and liquid in the tank, as well as new temperature and pressure.

As liquid $N_2O$ leaves the tank, some of the liquid inside the tank boils and turns to vapor. After a while, only saturated $N_2O$ vapor will remain inside the tank and it will no longer be possible to use the NHNE model. Thus, the fluid is considered compressible and further modeling is done to calculate the vapor mass flow ($\dot{m}_{v,out}$). While the flow is choked at the outlet area, the mass flow is calculated as:

$$\dot{m}_{oxi} = \dot{m}_{v,out} = A_{out} \cdot C_{d,out} \cdot \sqrt{\gamma \cdot P_{tank} \cdot \rho_v \cdot (\frac{2}{\gamma+1})^{(\gamma+1)/(\gamma-1)}} \tag{17}$$

As the vapor mass in the tank decreases, the pressure also decreases. At some point, the pressure inside the tank will not be enough for the flow to be choked. Thus, the $\dot{m}_{oxi}$ is calculated as:

$$\dot{m}_{oxi} = \dot{m}_{v,out} = A_c \cdot C_d \cdot \sqrt{\frac{2\gamma}{\gamma-1} \cdot \rho_v \cdot P_{tank} \cdot [(\frac{P_2}{P_{tank}})^{2/\gamma} - (\frac{P_2}{P_{tank}})^{(\gamma+1)/\gamma}]} \tag{18}$$

Where $P_{tank}$ is the pressure inside the oxidizer tank and $C_{d,out}$ is the tank-outlet discharge coefficient and $\dot{m}_{v,out}$ is the mass flow of vapor through the outlet.

## 3. RESULTS AND DISCUSSION

The current implementation of the described method presents a much more complete perspective on the operation of the engine compared to simple analytical approximations, and provides detailed data on the oxidizer tank and combustion chamber behavior. The simulated thrust response is presented in Figure 2, showing clearly the two-step behaviour due to the depletion of oxidizer in the liquid state. Maximum thrust happens right after ignition, when tank pressure is also maximum. This characteristic is specially beneficial to rocket stability at liftoff.

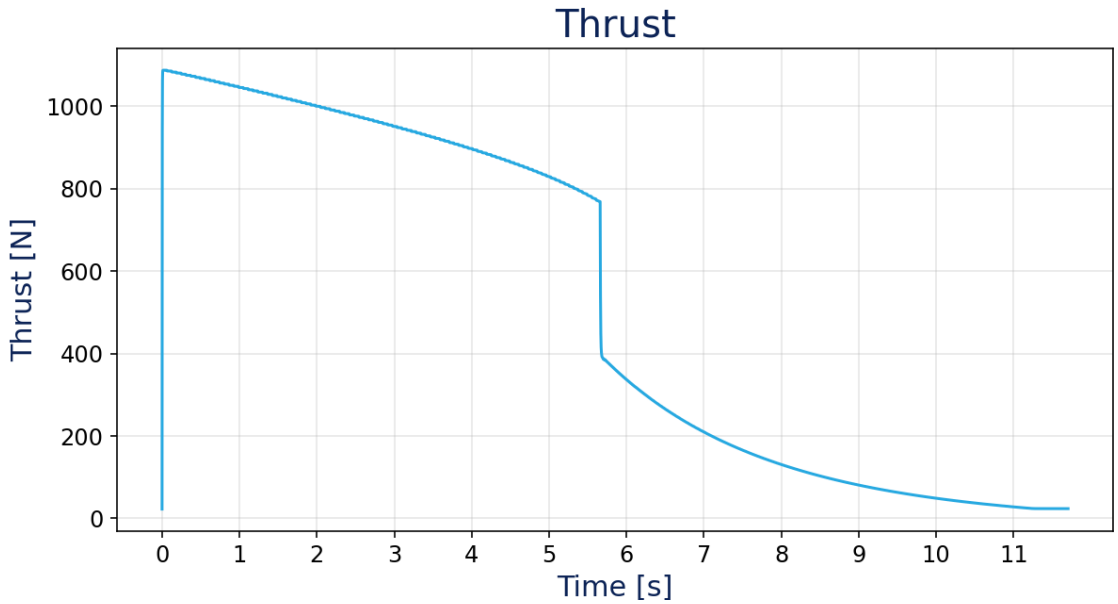


Figure 2. Gluon FT simulation results: Thrust.

Although the conceptual design considered a burn time of 5 seconds, *LP* depletion happens only at approximately $5.7\ s$. This extra burning time is actually beneficial to the design in general, since at the end of the *LP*, thrust is about $20\%$ lower than nominal.

Oxidizer mass during engine operation is presented in Figure 3, which shows vapor mass increasing while liquid is being consumed, confirming the self-pressuring aspect of Nitrous Oxide, together with the fact that at ambient temperature ($20°C$), presents a pressure of approximately $51\ bar$ (Jamieson and Beaton, 1991).

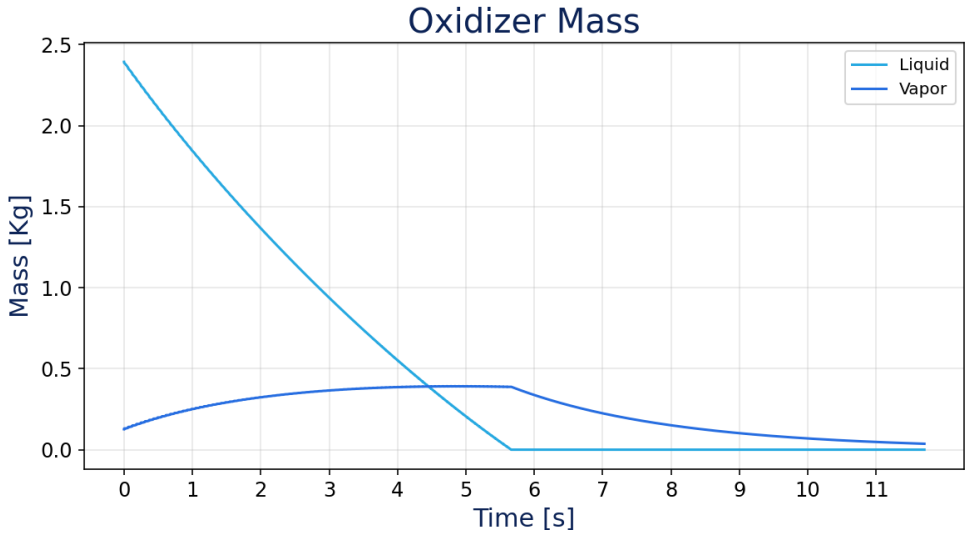


Figure 3. Gluon FT simulation results: Oxidizer Mass.

During the second phase, as soon as nitrous oxide vapor starts to be injected in the combustion chamber, there is a steep drop in characteristic velocity, as seen in Figure 5. Characteristic velocity, hence specific impulse, continues to drop in a linear fashion, accompanying the drop in pressure inside the oxidizer tank shown on the right side of the graph in Figure 4

| **Gluon FT - Simulation Results** | |
|---|---|
| Initial O/F | 5.11 |
| $t_b$ (LP) | 5.66 $s$ |
| $t_b$ (Overall) | 11.71 $s$ |
| Average $P_C$ (LP) | 322 $psi$ |
| Max. $P_C$ | 365 $psi$ |
| Average Thrust (LP) | 960 $N$ |
| Maximum Thrust | 1087 $N$ |
| Total Impulse | 6304 $N.s$ |
| Specific Impulse (Overall) | 198 $s$ |
| Specific Impulse (LP) | 215 $s$ |

Table 2. General Performance data from simulation results (LP: Oxidizer Liquid Phase).

From the data presented in Table 3, follows that performance results are satisfactory and meet the requirements of the conceptual design of the engine.

## 4. CONCLUSION

With the information and experience gathered from the presented simulations its possible to assess one of our objectives in this work, which is to evaluate the contribution of the "vapor phase" from an hybrid thruster.

Most of the total impulse delivered by the thruster occurs during the *LP*, in which the oxidizer is injected in the liquid phase. As soon as the liquid phase is depleted and $N_2O$ vapor starts to be injected, and there is a sudden drop on specific impulse, and an even larger drop in thrust due to the smaller oxidizer mass flow, however, this low-thrust profile extends

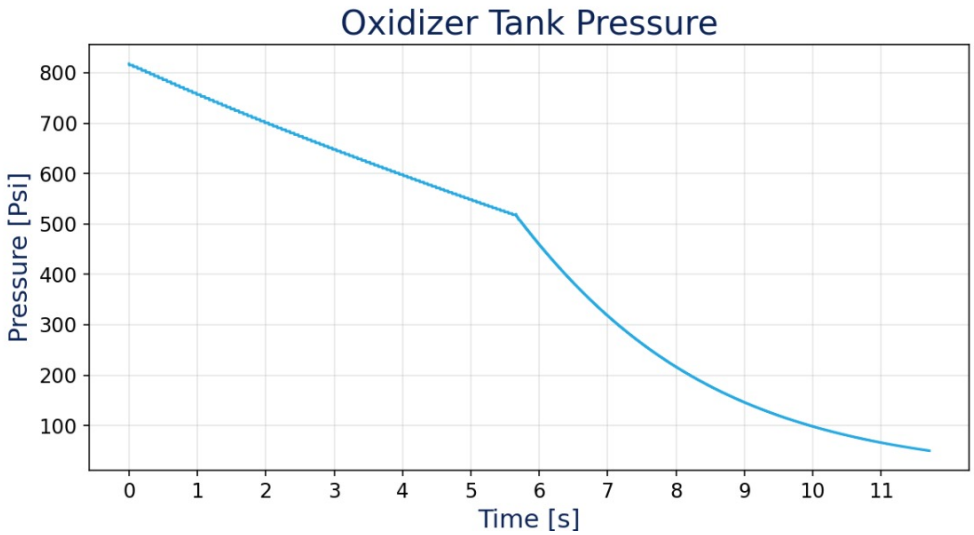


Figure 4. Gluon FT simulation results: Oxidizer Tank Pressure.

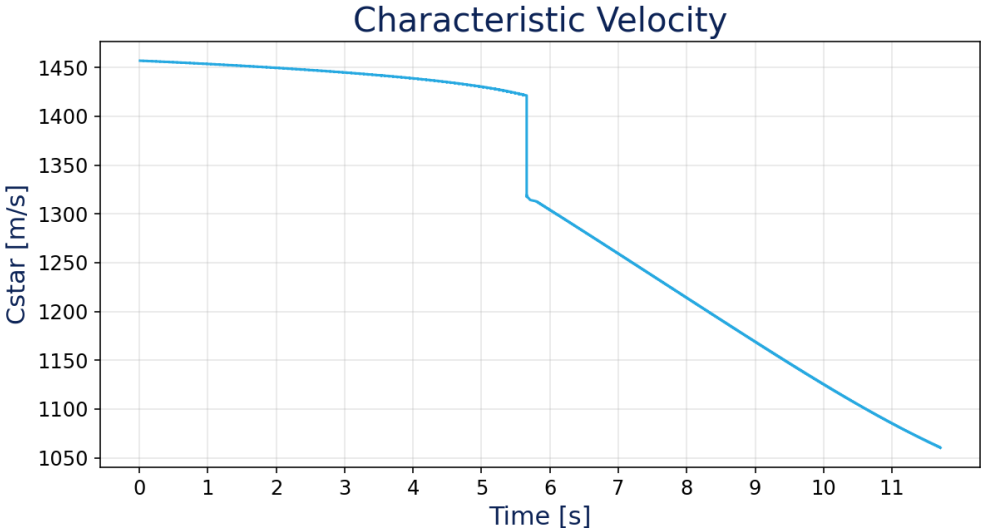


Figure 5. Gluon FT simulation results: Characteristic Velocity.

for a considerable amount of time, until the vapor is depleted. From this and the exposed in Figure 2, it is possible to conclude that both liquid and vapor phases contribute considerably to total impulse, although the first being the most important. Another remark about the *VP* is that the lower thrust and longer burn time of the vapor phase can have a considerable impact in thermal load of the engine and, if longer exposure to combustion temperatures due to the extended burn time are not accounted in thermal design, burn-throughs or other thermal fail modes can occur. This result confirms past experience with previous versions of the Gluon engine, with which the long burn time of the *VP* was decisive to the thermal liner design.

The developed software proved itself as a valuable tool to obtain more information about operation of our engines, providing much more detail and accuracy onto predicted engine operation characteristics. With this, many test readings from sensors on the test bench are much more streamlined to what is expected to happen in tests, and design modifications can be further compared and optimized.

Modeling and simulation makes its way together with safety culture to continue our history of successful developments and high performance, low cost propulsion represented by the Gluon family of thrusters. Continuous improvement of our products and ensured reliability backed by exhaustive testing makes our engines and vehicles ready to provide launches of educational payloads. In Figure 6, a picture of a Gluon engine test fire is shown.

Figure 6. Gluon engine test fire.

## 5. REFERENCES

Dyer, J., Zilliac, G., Sadhwani, A., Karabeyoglu, A. and Cantwell, B., 2007. "Modeling feed system flow physics for self-pressurizing propellants". In *43rd AIAA/ASME/SAE/ASEE Joint Propulsion Conference & Exhibit*. p. 5702.

Eilers, S.D. and Whitmore, S.A., 2008. "Correlation of hybrid rocket propellant regression measurements with enthalpy-balance model predictions". *Journal of Spacecraft and Rockets*, Vol. 45, No. 5, pp. 1010–1020.

Jamieson, D. and Beaton, C., 1991. "Thermophysical properties of nitrous oxide". *Journal of propulsion and Power*. URL `http://edge.rit.edu/edge/P07106/public/Nox.pdf`.

Sutton, G.P. and Biblarz, O., 2016. *Rocket propulsion elements*. John Wiley & Sons.

Waxman, B.S., Cantwell, B., Zilliac, G. and Zimmerman, J.E., 2013. "Mass flow rate and isolation characteristics of injectors for use with self-pressurizing oxidizers in hybrid rockets". In *49th AIAA/ASME/SAE/ASEE Joint Propulsion-Conference*, p. 3636.

Whitmore, S.A. and Chandler, S.N., 2010. "Engineering model for self-pressurizing saturated-n2o-propellant feed systems". *Journal of propulsion and Power*, Vol. 26, No. 4, pp. 706–714.

## 6. RESPONSIBILITY NOTICE

The authors are solely responsible for the printed material included in this paper.